Characterization of Wind Loading of the Large Radio Telescope

Sabine Upnere[1], Normunds Jekabsons[2], Roberts Joffe[3],
[1-3] *Engineering Research Institute 'Ventspils International Radio Astronomy Centre' of Ventspils University College*

***Abstract* – This paper describes numerical simulations of wind-loads on the large parabolic reflector antenna RT-32 with a diameter of 32 m and a methodology of how calculated wind pressure can be transferred to beam-based digital model. The wind flow leads to a compressive load on the dish and thus to a deformation of the reflector. These deformations can cause a performance degradation of the input signal, or even loss of the observed or controlled object. The calculations show that the wind induced force is small in comparison with gravitational loads. Studies have been carried out at the Ventspils International Radio Astronomy Centre (VIRAC) to investigate the wind-loading effects on the radio telescope RT-32 structure. The wind loads are calculated with the help of an open sourced Computational Fluid Dynamics toolkit OpenFOAM.**

***Keywords* – large radio telescope, Computational Fluid Dynamics, turbulence models, wind-load, Finite Element Model.**

I. Introduction

The RT-32 is a radio telescope with a reflector diameter of 32 m. The parabolic mirror can rotate about an azimuth and an elevation axis. The antenna system is of the Cassegrain type. Cassegrain antennas are dual-reflector systems with paraboloidal primary reflector and hyperboloidal secondary reflector [1].

In order to analyse the reflector surface precision perturbed by wind-loads the development of the Computational Fluid Dynamics (CFD) model is required. The CFD model is created by using coordinates of the reflector surface and beams of the tree-dimensional, beam-based digital model of the RT-32, which has been developed at VIRAC, see [2].

The geometrical dimensions of the antenna and the wind speed are the causes of the highly turbulent flow around the radio telescope. In order to correctly calculate the flow field, turbulence models are used. Two approaches are used in this work: Reynolds Averaged Navier-Stokes (RANS) models and Large-Eddy Simulations (LES).

The second part of the paper describes the transfer of the CFD results to beam-based digital model presented in [2]. In order to apply the force of wind-loads obtained from a Finite Volume Model to a Finite Element Model, the corresponding calculated pressure and coordinates of node points of reflector plates are used.

Consequently, combining wind induced loads with gravitational force a unified, liquid-solid interaction model of the RT-32 radio telescope is obtained.

II. Solution Strategy of the CFD

A. Computational domain and mesh generation

The computational domain of the RANS approach covers *10D* (*D* is the width of the tower building) in streamwise (*X*) direction (68 m < *x* < -272 m), *5D* in lateral (*Y*) direction (-85 m < *y* < 85 m) and *4H* (*H* is the height of the telescope) in vertical (*Z*) direction. The computational domain and coordinate definition for the LES are given in Fig. 1. The computational domain of the LES is 204 x 136 x 118 m^3 (length x width x height).

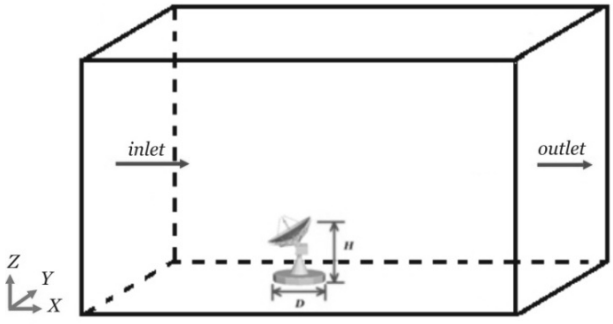

Fig. 1. Computational domain for the LES

The RT-32 Finite Volume Model contains the main reflector, a tower building, a frame and some of larger beams (see Fig. 2). Beams and the tower construction surface mesh are created with the open source tool Gmsh and then they are exported to triangulated surface format, which is used as an input file of the OpenFOAM's utility.

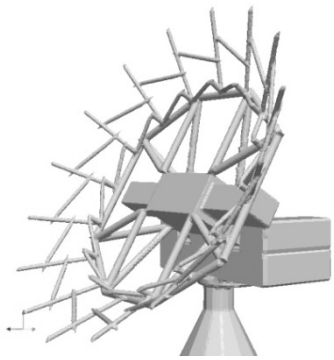

Fig. 2. Beams in the Finite Volume Model

The 3D mesh of the computational domain (see Fig. 3) is generated by use of hexahedra and spit-hexahedra cells. Starting from a coarse background mesh the new mesh is generated iteratively with a given level of refinement close to the surface.

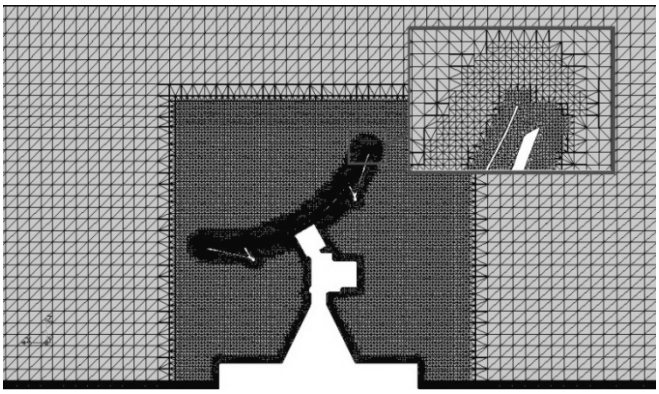

Fig. 3. The mesh of the computational domain

The characteristics of computational domains are summarized in Table 1.

TABLE I

CHARACTERISTICS OF COMPUTATIONAL DOMAINS

Model type	Cells	Maximum aspect ratio	Maximum skewness	Maximum non-ortogonality
RT-32, RANS	$2.23 \cdot 10^6$	10	5.05	56.79
RT-32, LES	$2.69 \cdot 10^6$	10	19.38	64.89

B. Turbulence models and numerical methods

The governing equations of incompressible Newtonian fluid consist of the mass conservation equation (1) and impulse conservation equations (2).

$$\frac{\partial u_i}{\partial x_i} = 0, \qquad i = 1,2,3 \tag{1}$$

$$\frac{\partial u_i}{\partial t} + \frac{\partial}{\partial x_j}\left(u_i u_j\right) = -\frac{1}{\rho}\frac{\partial p}{\partial x_i} + \nu \frac{\partial}{\partial x_j}\left(\frac{\partial u_i}{\partial x_j} + \frac{\partial u_j}{\partial x_i}\right) \tag{2}$$

in which $u=(u_1,u_2,u_3)$ is the velocity field, ρ *is* the density, p and ν are, respectively, the pressure and the kinematic viscosity [4]. The standard transport equations are used; see [6].

The Reynolds number (3) involved in the simulations is $\sim 10 \cdot 10^6$. In this study, the characteristic velocities are about 3.5 m/s, therefore the flow could be treated as a incompressible flow.

$$Re = \frac{L_C \cdot U_C}{\nu} \tag{3}$$

where L_C and U_C are characteristic length and velocity respectively.

Two RANS turbulence models are used in the present study: the standard k-ε model [3] and RNG k-ε model [4], where k is the turbulence kinetic energy and ε is its rate of dissipation.

A numerical study simulating the time-dependant flow fields is carried out using Large Eddy Simulation Models [5, 7].

In the LES it is required to solve the filtered Navier-Stokes equations with additional sub-grid scales (SGS) stress terms. If the variables of the incompressible Newtonian equations are subjected to the filtering operation, then

$$\frac{\partial \overline{u_i}}{\partial x_i} = 0 \tag{4}$$

$$\frac{\partial \overline{u_i}}{\partial t} + \frac{\partial}{\partial x_j}\left(\overline{u_i u_j}\right) = -\frac{1}{\rho}\frac{\partial \bar{p}}{\partial x_i} + \frac{\partial \tau_{ij}}{\partial x_j} + \frac{\partial \tau_{ij}^{SGS}}{\partial x_j} \tag{5}$$

where

$$\tau_{ij}^{SGS} = \overline{u}_i \overline{u}_j - \overline{u_i u_j} \tag{6}$$

τ_{ij}^{SGS} is the SGS Reynolds stress generally modelled using various SGS models [8]. In this study two SGS turbulence models are used: the k-equation and Smagorinsky SGS model.

Smagorinsky model is an eddy viscosity model, given as

$$\tau_{ij} - \frac{1}{3}\tau_{kk}\delta_{ij} = -2\nu_T \bar{S}_{ij} \tag{7}$$

where $\bar{S}_{ij}$ is the resolved strain rate tensor, δ_{ij} is the Kronecker delta, and ν_T is the eddy viscosity. The length scale is the filter width Δ, and the velocity scale is $\Delta|\bar{S}|$, where $\bar{S} = \sqrt{2\bar{S}_{ij}\bar{S}_{ij}}$ is a measure of the velocity gradient. The eddy viscosity in (7) is given by

$$\nu_T = (C_S \Delta)^2 |\bar{S}| \tag{8}$$

where C_S is the Smagorinsky constant [7].

The van Driest damping function near the solid boundary is used. The van Driest scaling reads

$$C_S = C_{s0}\left(1 - e^{-\frac{y^+}{A}}\right)^2 \tag{9}$$

where $C_{s0}=0.17$ is Lilly's constant, $A=25$ is the van Driest constant and y^+ is the non-dimensional distance from the wall

$$y^+ = \frac{u_\tau y}{\nu} \tag{10}$$

which determines the relative importance of viscous and turbulent phenomena. In (10), u_τ is the wall shear velocity and y is the vertical coordinate [5].

In a *k*-equation model, only the length scale is prespecified and the velocity scale can be taken as $\sqrt{k}$ where k is determined from a separate transport equation. In the -*k*-equation SGS model, the eddy viscosity can be given by

$$\nu_T = C\sqrt{k}\Delta \tag{11}$$

where C is the model constant [7]. In the *k*-equation model an additional transport equation for the SGS turbulent kinetic energy (12) is solved.

$$\frac{\partial}{\partial t}(k) + \frac{\partial}{\partial x_i}(u_i k) - \frac{\partial}{\partial x_i}\left(\nu_{Eff}\frac{\partial}{\partial x_i}(k)\right) = -BL - \frac{c_e k^{\frac{3}{2}}}{\Delta} \tag{12}$$

where $\nu_{Eff} = \nu_T + \nu$, B is the local SGS stresses and L is Leonard stresses, c_e is the model coefficient. The last term on the right side corresponds to turbulent dissipation [9].

The Semi-Implicit Method for Pressure-Linked (SIMPLE) algorithm is used in the RANS for the pressure-momentum coupling. The Pressure Implicit with Splitting of Operators (PISO) method is used for LES calculations to solve the Navier-Stokes equations in unsteady problems.

The convergence is warranted by the normalized residual drop to 10^{-5} for all variables except the pressure, where the residual is smaller than 10^{-6}. The computations are performed on a cluster at the VIRAC. A total of 4 processors are used in parallel for simulations.

C. Boundary conditions

To describe the inflow velocity profile, the average measured wind speed u_{calc} (see [10]) and the average maximum wind speed u_{op} at which the radio telescope can be operated are used. At 50 m (the radio telescope RT-32 is ~50 m height) u_{calc}=4.61 m/s and u_{op}=17.5 m/s.

The expression of the logarithmic law is used to describe the velocity profile (13) of the atmospheric boundary layer.

$$u(z) = \frac{u_*}{\kappa}\ln\left(\frac{z}{z_0}\right) \tag{13}$$

where $u(z)$ is the wind speed at the height z, u_* - the friction velocity, κ is the von Karman constant (0.4187) and the aerodynamic roughness length, z_0, is the height above the ground where the flow velocity is zero.

The turbulence kinetic energy and the energy dissipation rate at the inlet for the RANS are calculated according to the following equations:

$$k_{inlet} = \frac{3}{2}(U_a I)^2 \tag{14}$$

$$\varepsilon_{inlet} = \frac{u_*^3}{\kappa(z+z_0)} \tag{15}$$

where U_a is the mean velocity at the inlet, I is the turbulence intensity.

The pressure p at the inlet is defined as a zero-gradient condition *(∂p/∂n=0)*.

At the outlet, the zero-gradient conditions are applied for all variables except the pressure, which is set to zero.

Telescope surface and ground is defined as wall, a zero-gradient condition is set for p, k and ε and non-slip condition (a value of (0,0,0) is fixed at the wall) is set for U by standard OpenFOAM wall-function [11]. The distance from the wall measured in viscous lengths is defined as

$$y^+ = \frac{u_* x_i}{\nu} \tag{16}$$

where x_i is coordinate. The dimensionless streamwise velocity is defined as follows

$$u^+ = \frac{1}{\kappa}\ln(Ey^+) \tag{17}$$

where E is a constant.

At the other boundaries, all variables are set to a slip condition: for a scalar it represents a zero-gradient condition and for a vector, the normal component is fixed to zero and the tangential components are zero-gradient. The exception is the pressure which is defined as a zero-gradient condition.

At the inlet and outlet boundaries in the LES models, the velocity is set to a cyclic condition, it enables two boundaries to be treated as if they are physically connected. The implementation of a routine to keep the mass flow rate in the domain constant is used. This is achieved by calculating the averaged mass flow rate at each time step and by consequently adapting the pressure gradient to keep it fixed.

For velocity values at the walls fixed values of (0,0,0) are used. The other boundaries are defined as symmetry planes. Van Driest damping functions is selected for a wall treatment.

III. Application of the CFD results in FEM

A. Description of the main reflector in models

The main reflector of the RT-32 radio telescope consists of 896 plates; the thickness of plates is 2 mm. The reflector in the Finite Volume Model is described as a boundary, see Fig 4a. The surface of the reflector is divided in rectangles, see Fig 4b.

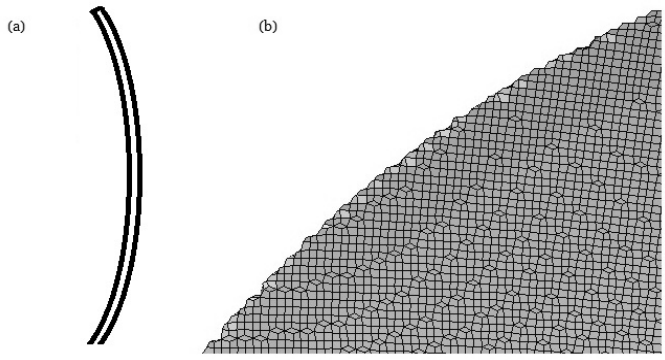

Fig. 4. The representation of the main reflector in the Finite Volume Model; the cross-section (a) and the surface (b) of the main reflector

Each plate of the reflector is connected to a support structure with four screws. The plate is represented using coordinates of these four points in the beam-based model. These coordinates are used to find corresponding points in the Finite Volume Model.

B. Detection of the wind force

In order to calculate a force with which the wind acts on the plate, an average pressure on both sides of the plate should be determined from the CFD model. The centre of each plate is defined from coordinates of points from the beam-based model where reflector plates are introduced.

A pressure on surface mesh elements is known from CFD calculations. Mesh elements near the centre of each reflector plate is detected. A distance between a plate centre and distal mesh element is chosen so that the average pressure does not differ significantly from CFD results (see Fig. 5).

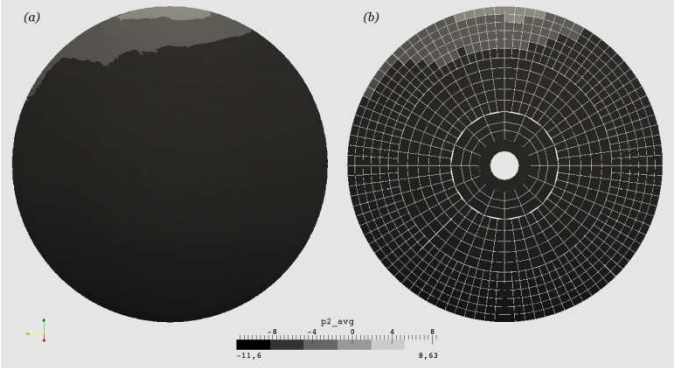

Fig. 5. Comparison of the pressure on a reflector in the CFD model (a) and average pressure on plates (b)

Considering that the plate is represented as a boundary in the CFD model then average pressure is calculated separately for both sides of the plate. The normal vectors are used to achieve separation (see Fig. 6). The normal vectors of surface mesh elements (n_1, n_2) are directed to boundary inside. The plate normal vector (n_{pl}) is opposite to the wind direction. The direction of surface normal vectors is compared with the plate normal vector and in that way sides are separated.

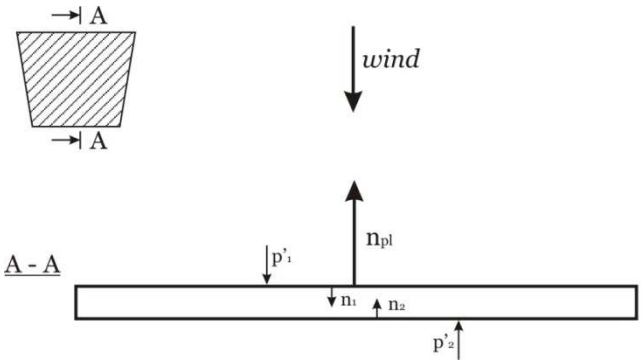

Fig. 6. The cross-section of the plate with normal vectors

The average pressure in the centre of the plate is found as follows:

$$\Delta_p = (p'_1 - p'_2)\rho \tag{18}$$

where p'_1 is the pressure on one side at the centre of the plate and p'_2 is on the other side. OpenFOAM calculates reduced pressure using (19) therefore (18) is multiplied by ρ.

$$p'_i = \frac{p}{\rho}, \qquad i = 1,2 \tag{19}$$

The wind induced force on the plate is calculated by

$$F_i = \Delta_p \cdot n_i, \quad i = 1,2,3 \tag{20}$$

where n_i is the corresponding component of the plate area normal vector. In order to get the force on each of the corner points of the plate calculated force (F_i) is divided by four.

IV. Results and Discussion

A. Parametric study of the CFD model

First series of CFD simulations are performed in a three-dimensional, empty (without a reflector, a tower building, a frame and beams) computational domain. Well fitted turbulence model gives constant x coordinate direction (wind direction), thus the main objectives for these simulations are:

- explore the effect of mesh roughness studies;
- extract the most convenient model constants for flow around the telescope.

Totally, four meshes (M1, M2, M3 and M4) are generated for the analysis of the mesh sensitivity. The number of cells M1, M2, M3 and M4 is approximately $0.33 \cdot 10^6$, $0.45 \cdot 10^6$, $0.90 \cdot 10^6$ and $1.8 \cdot 10^6$ respectively. The mesh M4 is used for simulations.

Three different roughness lengths z_0 (see (13)) are investigated for the RANS approach: z_0 = 0.001 m, z_0 = 0.01 m, z_0 = 0.1 m. The best conformity of the calculated profiles (see Fig. 7) with wind speed measurements gives the case when z_0 = 0.1 m and it is used for further simulations.

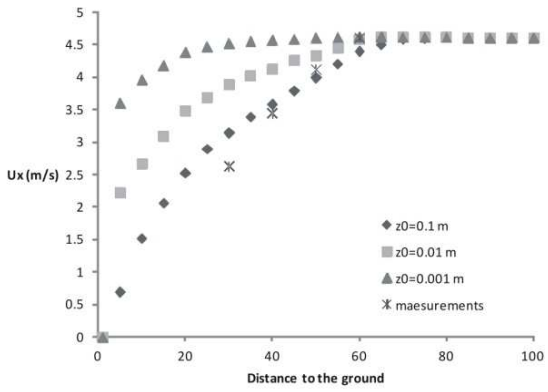

Fig. 7. The reduced pressure comparison for different meshes.

As the LES simulations are unsteady, the time step is chosen pertaining to the Courant number (see Fig. 8) conditions, which is defined for one cell as:

$$Co = \frac{|U|\Delta t}{\delta x} < 0.3 \tag{21}$$

where $|U|$ represents the magnitude of the velocity through that cell and δx is the cell size in the direction of the velocity. Δt is the time step used for simulations.

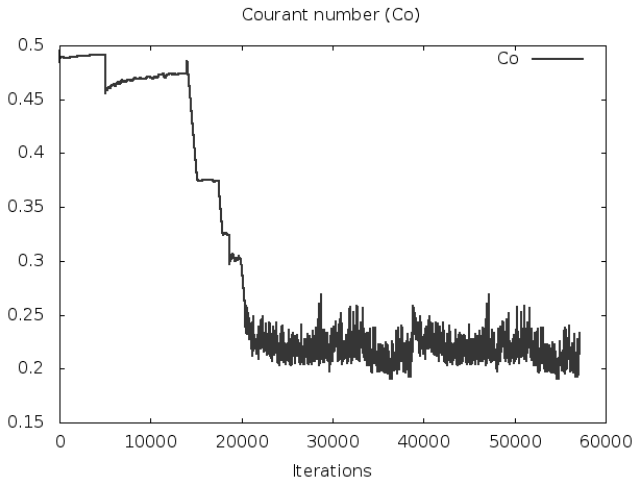

Fig. 8. Changes of Courant number with respect to time

B. Comparison between different elevation angles and wind directions

The CFD calculations of the RANS are made at four different elevation angles of the main reflector: α = 90° (zenith), 60°, 30°, 0° and at five wind directions (with respect to the surface of the dish): β = 0°, 45°, 90°, 135° and 180°. All elevation angles and wind directions used are shown in Fig.9. The inlet velocity (wind) is oriented in the *x*-direction. For the LES two elevation angles (α = 90° and 60°) and one wind direction (β = 0°) are used.

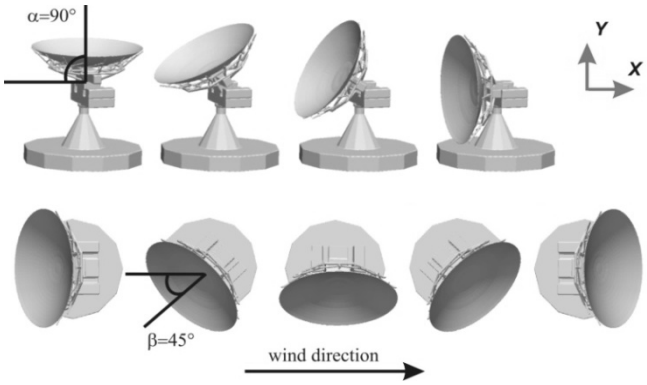

Fig. 9. Elevation angles and wind directions

The maximum pressure difference on the main reflector surface is in case when the wind direction is 45° and the elevation angle is 30° (see Fig. 10). RNG *k*-ε model and u_{calc} is used.

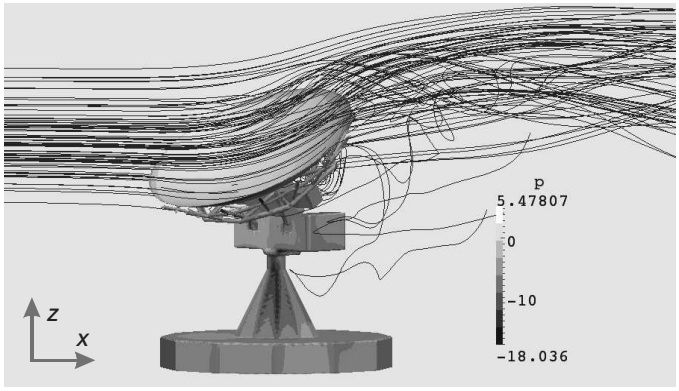

Fig. 10. The distribution of the pressure on a surface and a flow around the radio telescope. The wind direction is 45°, the elevation angle is 30°

In order to find the lift (F_L) and drag (F_D) force, the lift and drag coefficients (C_L and C_D) are calculated during the CFD simulations.

RANS calculations results (the RNG *k*-ε turbulence model is used) of the lift and drag coefficients for different cases are listed in Table 2 and Table 3 respectively. The lift and drag coefficients of LES calculations (Smagorinsky SGS model is used) are shown in Table 4. The u_{calc} wind speed is used for these calculations.

TABLE II

LIFT COEFFICIENTS C_L (RANS)

Elevation angle (°)	Wind direction (°)				
	0	45	90	135	180
90	0.779	-	-	-	-
60	-1.329	-1.047	0.137	0.258	0.744
30	-0.647	-0.663	0.167	0.031	0.078
0	0.004	0.006	0.014	-0.003	-0.003

TABLE III

DRAG COEFFICIENTS C_D (RANS)

Elevation angle (°)	Wind direction (°)				
	0	45	90	135	180
90	0.462	-	-	-	-
60	0.750	0.496	0.346	0.284	1.342
30	1.052	0.724	0.307	0.230	0.320
0	1.073	0.840	0.384	0.290	0.456

TABLE IV

LIFT AND DRAG COEFFICIENTS (LES)

Coefficients	Elevation angle (°)	Wind direction (0°)
C_L	90	0.773
C_L	60	-0.831
C_D	90	0.481
C_D	60	0.570

The lift force is obtained from

$$F_L = \frac{1}{2}\rho U_c^2 A C_L \tag{22}$$

where ρ the mass density of air, A is the reference area. The reference area is defined as the area of the projection of the object on a plane perpendicular to the direction of motion. The area is changed depending on the angle of attack. Similarly the drag force is obtained

$$F_D = \frac{1}{2}\rho U_c^2 A C_D \tag{23}$$

The lift and drag forces reach maximum at the elevation angle 30° and wind direction 0°. The lift force is 18% and the drag force is 11% of antenna own weight (P_g=637 [kN]) when wind speed corresponds to u_{op}.

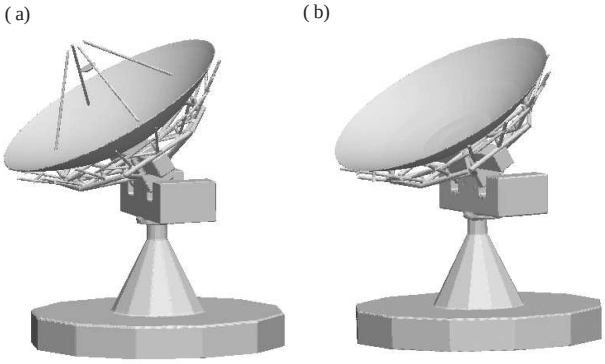

Fig. 11 The model with (a) and without (b) secondary reflector

The comparison of results of RANS and LES models demonstrates that the total wind force of the LES is 1% higher than calculated results using the RANS when elevation angle is 90°. Table 2, Table 3 and Table 4 show that difference between RANS and LES increases when elevation angle is 60°, it may be because the model contains secondary reflector in the LES case (Fig. 11a), but RANS model is without secondary reflector, see Fig 11b. Secondary reflector contains additional beams what change flow field.

C. Calculated wind force on the main reflector

The case, when the lift and drag forces reach maximum, is chosen for further studies, i.e. the elevation angle is 30° and wind direction is 0°. The RNG k-ε turbulence model is employed. In this case the pressure is calculated using u_{calc}. In order to get the operational pressure (wind speed is u_{op}) scaling factor is used. The scale factor is proportional to the square of the wind speed.

The reduced operational pressure is shown in Fig 12. The average reduced pressure on plates is within the interval of 61 m^2/s^2 to 197 m^2/s^2.

As seen in Fig. 12 the operational pressure is not symmetric, although one of k-ε turbulence models is used. The reason of asymmetry is representation of antenna supporting structure in the model. Fig. 2 shows that medium beams what join radial beams are not symmetrically placed.

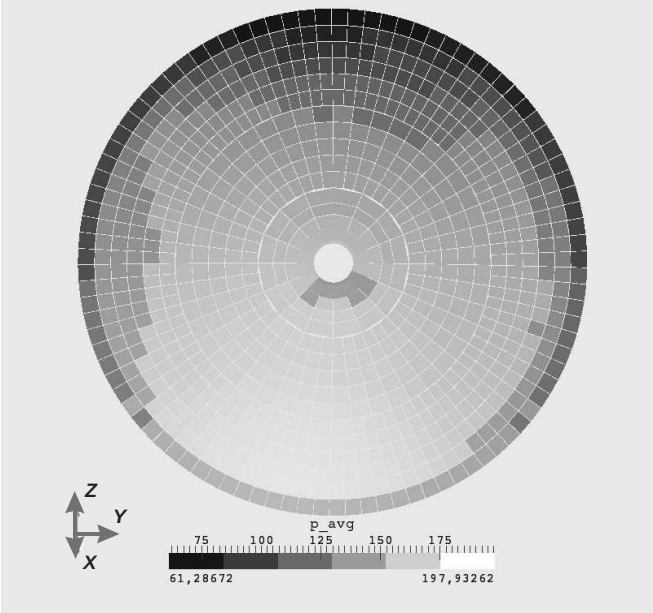

Fig. 12. Reduced operational pressure on main reflector plates

The total drag and lift forces are 117.37 kN and -71.32 kN respectively. Wind induced operational force on the main reflector plates obtained by (20) multiplied by scaling factor is shown in Fig. 13. Some rapid changes in radial values can be seen in Fig. 13, this can be explained by changes of the area of the plates. The maximum local force is approximately 387 N on the plate. The results obtained from Finite Element model (describe in [2]) show that the operational force causes maximum displacements of surface of about 5 mm which is approximately 10 times smaller than displacements due to gravitation.

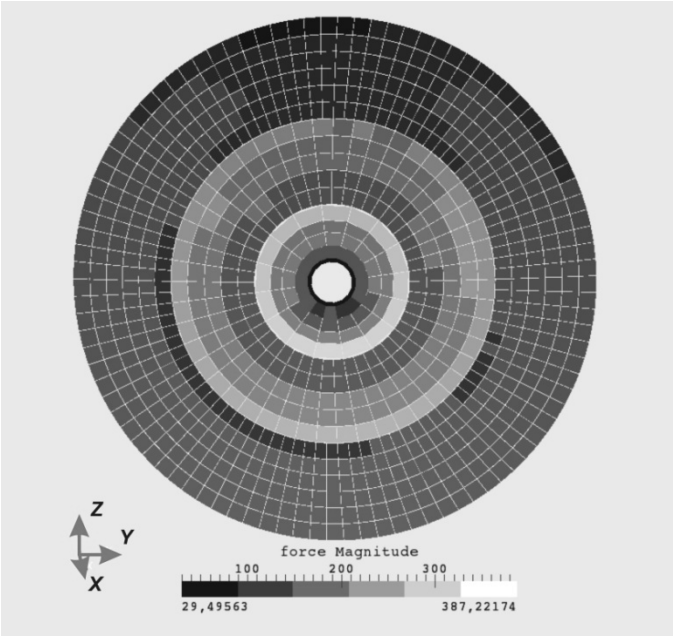

Fig. 13. Wind force on main reflector plates

V. CONCLUSIONS

Two approaches (Reynolds Averaged Navier-Stokes and Large-Eddy Simulations) are applied to predict the flow around the radio telescope RT-32 of simplified geometry case.

The results for 18 different cases in total are obtained, with five wind directions and four elevation angles. The minimum lift coefficient is at the elevation angle of 60° and wind direction 0°. The maximum drag coefficient is found for elevation angle 60° and wind direction 180°.

The difference between results of two RANS turbulence models (standard k-ε and RNG k-ε model) is 6.1% and 5.5% between two LES turbulence models (k-equation and Smagorinsky respectively) when u_{calc} wind speed is used.

Comparison of results of all computed CFD cases shows that the lift and drag forces reach maximum at the elevation angle 30° and wind direction 0°. In this case, when wind speed corresponds to u_{op} and operational force is used, the total force is F = (117.37; -0.003; -71.32) kN.

The maximum operational force induced by wind on one reflector plate reaches maximum of approximately 387 N, at u_{op}.

The CFD calculations show that maximum operational wind load acting on the reflector structure when velocity u_{op} is on the level of 21% of the gravitation force and it is rather significant and should not be neglected.

ACKNOWLEDGEMENTS

This research was funded by the European Social Fund (project No. 2009/0231/1DP/1.1.1.2.0/09/APIA/VIAA/151).

REFERENCES

[1] C.A. Balanis, Antenna theory. Analysis and Design, New Jersey: John Wiley & Sons, 2005, p. 1117

[2] S. Upnere, N. Jekabsons, R. Joffe, Analysis of Structural Integrity of Large Radio Telescopes Subjected to Gravitational and Wind loads, Lecture Notes in Information Technology, Vol. 25, 2012, pp. 148-154

[3] B.E. Launder and D.B. Spalding, The numerical computation of turbulent flows, Computer Methods in Applied Mechanics and Engineering, Vol. 3, 1974, pp. 269-289

[4] V. Yakhot et all, Development of turbulence models for shear flows by double expansion techniques, Physics of Fluids, Vol. A4, 1992, pp. 1510-1520

[5] P. Sagaut, Large Eddy Simulation for Incompressible Flows, Berlin: Springer, 2006, p. 557

[6] S. Upnere et al., Analysis of wind influence to radio astronomy observations at Irbene radio telescope complex, Scientific Journal of RTU, Vol. 6, 2011, pp. 118-126

[7] X. Jiang and C.-H. Lai, Numerical Techniques for Direct and Large-Eddy Simulations, London: CRC Press, 2009, p. 264

[8] O. C. Zienkiewicz et al., The Finite Element Method for Fluid Dynamics, London: Elsevier BH, 2009, p. 435

[9] E. de Villiers, The Potential of Large Eddy Simulation for the Modeling of Wall Bounded Flows, PhD thesis, Imperial College of Science, 2006, p. 375

[10] V. Bezrukovs, Vl. Bezrukovs, N. Levins, Problems in assessment of wind energy potential and acoustic noise distribution when designing wind power plants, Scientific Journal of RTU, Vol. 6, 2011, pp. 9-16

Normunds Jekabsons, PhD, Ventspils University College, The Engineering Research Institute "Ventspils International Radio Astronomy Centre" (VIRAC).
Dr Normunds Jekabsons is a senior researcher at VIRAC. Since 2010, he is the head of high performance computing division at VIRAC. The main research areas are Computational Fluid Dynamics, data processing and solid mechanics. Title of his doctoral thesis was "Mechanics of composites with fiber bundle meso-structure", from Luleå University of Technology (Sweden), year 2002. After finishing PhD studies in Sweden (1998-2002), Normunds Jekabsons has continued his professional work in Latvia. During the last nine years he has participated in several local and international research and engineering projects.
Address: Inženieru-101, LV-3605, Ventspils, Latvia
Phone: +371 26141530
E-mail: normundsj@venta.lv

Roberts Joffe, PhD, Professor, Luleå University of Technology (LTU), senior researcher at VIRAC.
Dr Roberts Joffe has been working at LTU as auniversity lecturer since 2002 and in 2012 was appointed Professor. The main research area is mechanics of composites, in particular, mechanisms governing mechanical properties of polymer composites. He has participated in a number of national projects as well as in large EC funded projects related to the development of advanced polymer composites and development of nano- and natural composites. He has published 37 papers in international journals and more than 30 contributions in conference proceedings. He has received MSc in Physics from the University of Latvia in 1993; Tech. Lic. in Engineering from LTU in 1996; Ph.D. and Docent degree in Polymeric Composite Materials from LTU in 1999 and 2007 respectively.
Address: Lulea University of Technology, SE-97187, Lulea, Sweden
Phone: +46 920 491940
E-mail: Roberts.Joffe@ltu.se

Sabine Upnere, Mg. sc. comp., researcher, Ventspils University College, The Engineering Research Institute "Ventspils International Radio Astronomy Centre".
Sabine Upnere has been a researcher since 2009. Her main research area and interest is the Computational Fluid Dynamics. She regularly takes part in local and international scientific conferences. She received her Bachelor's Degree at Liepaja Pedagogical Academy and Master's Degree at Ventspils University College in 2004 and 2009 respectively.
Address: Inženieru-101, LV-3605, Ventspils, Latvia
Phone: +371 26585324
E-mail: sabineu@venta.lv